Spatial Coordination Of Stomatal Patterning Between Leaf Surfaces In Amphistomatous *Arabidopsis thaliana* Incurs No Photosynthetic Advantage

Jacob L. Watts

??Colgate University

jwatts@colgate.edu

*

Graham Dow

??ETH

graham.dow@usys.ethz.ch

Thomas N. Buckley

??University of California Davis

tnbuckley@ucdavis.edu

†

Christopher D. Muir

??University of Hawaii at Manoa

cdmuir@hawaii.edu

†

September 27, 2023

Abstract

This is the abstract.

It consists of two paragraphs.

1 Introduction

Stomatal anatomy (e.g. size, density, distribution, and patterning) and movement regulate gas exchange during photosynthesis, namely CO_2 assimilation and water loss through transpiration. Since waxy cuticles are mostly impermeable to CO_2 and H_2O, stomata are the primary entry points through which gas exchange occurs despite making up a small percentage of the leaf area (Lange et al. 1971). Stomata consist of two guard cells which open and close upon changes in turgor pressure or hormonal cues (McAdam and Brodribb 2016). The stomatal pore leads to an internal space known as the substomatal cavity where gases contact the mesophyll. Once in the mesophyll, CO_2 diffuses throughout a network of intercellular air space (IAS) and into mesophyll cells where CO_2 assimilation (A) occurs within the chloroplasts (Lee and Gates 1964). Stomatal conductance and transpiration are determined by numerous environmental and anatomical parameters such as vapor pressure deficit (VPD), irradiance, temperature, wind speed, leaf water potential, IAS geometry, mesophyll cell anatomy, and stomatal anatomy.

Many successful predictions about stomata and other leaf traits can be made by hypothesizing that natural selection should optimizes CO_2 gain per unit of water loss (Cowan and Farquhar 1977; Buckley, Sack, and Farquhar 2017; Sperry et al. 2017). However, stomatal anatomy may be partially constrained by physical and developments limits on phenotypic expression (Croxdale 2000; Harrison et al. 2020; Christopher D. Muir et al. 2023). Sometimes optimization leads to similar phenotypes across many disparate species. For example, almost all stomata follow the one cell spacing rule to maintain proper stomatal functioning (Geisler, Nadeau, and Sack 2000; Dow, Berry, and Bergmann 2014); however some species (notably in *Begonia*) appear to benefit from overlapping vapor shells caused by stomatal clustering (Yi Gan et al. 2010; Lehmann and Or 2015; Papanatsiou, Amtmann, and Blatt 2017). Stomatal traits also vary adaptively in different environments. Stomatal density positively co-varies with irradiance during leaf development and negatively co-varies with CO_2 concentration (Gay and Hurd 1975; Schoch, Zinsou, and Sibi 1980; Woodward 1987; Royer 2001), consistent with optimality predictions. Stomatal size is jointly controlled by genome size, light, and stomatal density (Jordan et al. 2015). Size positively co-varies with genome size (Roddy et al. 2020) and negatively co-varies with stomatal density (Camargo and Marenco 2011). Total stomatal area (size × density) is optimized for operational conductance ($gs_{s,op}$) rather than maximum conductance ($gs_{s,max}$) such that stomatal apertures are most responsive to changes in the environment at their operational aperture (Franks et al. 2012; Liu et al. 2021). Stomatal aperture can compensate for maladaptive stomatal densities to an extent (Büssis et al. 2006), but stomatal density and size ultimately determine a leaf's

---

*Corresponding author; Email: jwatts@colgate.edu

†**??**1

2

theoretical $gs_{s,max}$ (Sack and Buckley 2016), which is proportional to $gs_{s,op}$ (Murray et al. 2020). Additionally, low stomatal densities lead to irregular and insufficient CO_2 supply and reduced photosynthetic efficiency in areas far from stomata (Roland Pieruschka et al. 2006; Morison et al. 2005), while high stomatal densities can reduce water use efficiency (WUE) (Büssis et al. 2006) and incur excessive metabolic costs (Deans et al. 2020). In most species, stomata occur on the abaxial (usually lower) leaf surface; but amphistomy, the occurrence of stomata on both abaxial and adaxial leaf surfaces, is also prevalent in high light environments with constant or intermittent access to sufficient water (Mott, Gibson, and O'Leary 1982; Jordan, Carpenter, and Brodribb 2014; Christopher D. Muir 2018; Drake et al. 2019; Christopher D. Muir 2019). Amphistomy effectively halves the CO_2 diffusion path length and boundary layer resistance by doubling boundary layer conductance (Parkhurst 1978; Harrison et al. 2020; Mott and Michaelson 1991). Historically, stomatal patterning in dicot angiosperms was thought to be random with an exclusionary distance surrounding each stomate (Sachs 1974); however, the developmental controls of stomatal patterning are poorly understood and likely more complex than random development along the leaf surface. Croxdale (2000)] reviews three developmental theories which attempt to explain stomatal patterning in angiosperms: inhibition, cell lineage, and cell cycle, ultimately arguing for a cell cycle based control of stomatal patterning.

The patterning and spacing of stomata on the leaf affects photosynthesis in C_3 leaves by altering the CO_2 diffusion path length from stomata to sites of carboxylation in the mesophyll. Maximum photosynthetic rate (A_{max}) in C_3 plants is generally co-limited by biochemistry and diffusion, but modulated by light availability (Parkhurst and Mott 1990; Manter 2004; Carriquí et al. 2015). Low light decreasing CO_2 demand by limiting electron transport rate, leading to relatively high internal CO_2 concentration (C_i) and low A_{max} (Kaiser et al. 2016). In contrast, well hydrated leaves with open stomata in high light, photosynthesis is often limited by CO_2 supply as resistances from the boundary layer, stomatal pore, and mesophyll can result in insufficient COC_2 supply at the chloroplast to maxmimize photosynthesis (Farquhar, Caemmerer, and Berry 1980; Lehmeier et al. 2017). In this study, we focus primarily on how stomatal patterning affects diffusion, ignoring boundary layer and mesophyll resistances.

To maximize CO_2 supply from the stomatal pore to chloroplasts, stomata should be uniformly distributed in an equilateral triangular grid on the leaf surface so as to minimize stomatal number and CO_2 diffusion path length (Parkhurst 1994). As the diffusion rate of CO_2 though liquid is approximately $10^4\times$ slower than CO_2 diffusion through air, mesophyll resistance is generally thought to be primarily limited by liquid diffusion (Aalto and Juurola 2002; Evans et al. 2009), but diffusion through the IAS has also been shown to be a rate limiting process because the tortuous, disjunct nature of the IAS can greatly increase diffusion path lengths (Harwood, Théroux-Rancourt, and Barbour 2021). Additionally, tortuosity is higher in horizontal directions (parallel to leaf

surface) than vertical directions (perpendicular to leaf surface) because of the cylindrical shape and vertical arrangement of pallisade mesophyll cells (Earles et al. 2018; Harwood, Théroux-Rancourt, and Barbour 2021). However, the ratio of lateral to vertical diffusion rate is still largely unknown (Morison et al. 2005; R. Pieruschka 2005; Roland Pieruschka et al. 2006). Depending on the thickness of the leaf, porosity of the leaf mesophyll, tortuosity of the IAS, and lateral to vertical diffusion rate ratio, minimizing diffusion path length for CO_2 via optimally distributed stomata may yield significant increases in CO_2 supply for photosynthesis and higher $A_{\max}$.

We hypothesized that natural selection will favor stomatal patterning and distribution to minimize the diffusion path length. In amphistomatous leaves, this would be accomplished by 1) a uniform distribution of stomata on both abaxial and adaxial leaf surfaces and 2) coordinated stomatal spacing on each surface that offsets the position of stomata (Fig. **??**). Coordination between leaf surfaces is defined in this study as the occurrence of stomata in areas farthest from stomata on the opposite leaf surface. Additionally, because CO_2 is more limiting for photosynthesis under high light, we hypothesize that in high light 3) there should be more stomata, and 4) stomata should be more uniformly distributed than in low light. Finally, as stomatal densities are selected for optimal operational aperture, we hypothesize that 5) stomatal length will be positively correlated with the area of the leaf surface to which it is closest. We refer to this as the 'stomatal zone', the leaf area surrounding a focal stomate closest to that stomate and therefore the zone it supplies with CO_2). This way, each stomate can be optimally sized relative to the mesophyll volume it supplies.

To test these hypotheses, we grew the model plant *Arabidopsis thaliana* in high, medium, and low light and measured stomatal density, size, and patterning on both leaf surfaces, and spatial coordination between them. We use Voronoi tessellation techniques to calculate stomatal zones. We also used a 2-D porous medium approximation of CO_2 diffusion and photosynthesis to predict the photosynthetic advantage of optimal versus suboptimal coordination in stomatal coordination between surfaces. Specifically, we predicted that traits which affect diffusion path length (leaf thickness, stomatal density, leaf porosity, lateral-vertical diffusion rate ratio), diffusion rate (temperature, pressure), and CO_2 demand (Rubisco concentration, light) would modulate the advantage of optimal stomatal arrangement following the relationships outlined in Table 2. Here, we integrate over reasonable parameter space to determine the ecophysiological context most likely to favor stomatal spatial coordination in amphistomatous leaves.

4

2 Materials and methods

2.1 Data Preparation

[CDM: Graham Dow provided these images. We'll need to add him as a co-author and ask him to write methods on image acquisition.]

Arabidopsis thaliana plants were grown in three different light environments: low light (50 PAR), medium light (100 PAR), and high light (200 PAR) following the light standards from (CITE). Once leaves were mature, we captured images of the abaxial and adaxial leaf surfaces using xxx bifocal microscope. This microscope allows the capture of two focal lengths that are spatially correlated such that pixel (1,1) of the abaxial surface image is directly above pixel (1,1) of the adaxial surface image, and so on… Images were 512 by 512 pixels and covered X leaf surface area. We captured 132 images in total, making 66 abaxial-adaxial image pairs. The position of all stomata were recorded using ImageJ (Schneider, Rasband, and Eliceiri 2012).

2.2 Single Surface Analysis

We tested whether stomata are non-randomly distributed by comparing the observed stomatal patterning to a random uniform pattern. For each leaf surface image with n stomata we generated 10^3 synthetic surfaces with n stomata uniformly randomly distributed on the surface. For each sample image, we compared the observed Nearest Neighbor Index (NNI) to the null distribution of NNI values calculated from the synthetic data set. The observed stomatal distribution is dispersed relative to a uniform random distribution if the observed NNI is greater than 95% of the synthetic NNI values (one-tailed test).

NNI is the ratio of observed mean distance ($\overline{D}_O$) to the expected mean distance ($\overline{D}_E$) where $\overline{D}_E$ is:

$$\overline{\mathrm{D}}_{\mathrm{E}} = \frac{0.5}{\sqrt{A_l/n_{\mathrm{stomata}}}} \tag{1}$$

A_l is leaf area and n_{stomata} the number of stomata. $\overline{D}_E$ is the theoretical average distance to the nearest neighbor of each stomate if stomata were randomly distributed (CITE; Clark and Evans, 1954). And $\overline{D}_O$ calculated for each synthetic data set is:

$$\overline{\mathrm{D}}_{\mathrm{O}} = \frac{\sum_{i=1}^{n_{\mathrm{stomata}}} d_i}{n_{\mathrm{stomata}}} \tag{2}$$

d_i is the distance between stomate$_i$ and its nearest neighbor. We calculated NNI using the R package **spatialEco** version 2.0.1.

For each sample image, we also simulated 10^3 synthetic data with n stomata ideally dispersed in an equilateral triangular grid. For these grids, we integrated over plausible

stomatal densities and then conditioned on stomatal grids with exactly n stomata. The simulated stomatal count was drawn from a Poisson distribution with the mean parameter λ drawn from a Gamma distribution with shape n and scale 1 $\lambda \sim \Gamma(n, 1)$. $\Gamma(n, 1)$ is the posterior distribution of λ with a flat prior distribution. This allows us to integrate over uncertainty in the stomatal density from the sample image.

We calculated the dispersion index DI) which varies from zero to one. Zero is uniformly random and one is ideally dispersed:

$$\text{DI} = \frac{\text{NNI} - \text{median}(\text{NNI}_{\text{random}})}{\text{median}(\text{NNI}_{\text{uniform}}) - \text{median}(\text{NNI}_{\text{random}})} \tag{3}$$

Uniformly distributed stomata on a leaf with stomatal density (D_S) maximize $\overline{D}_O$ in an equilateral triangle pattern with side lengths (s) equal to two times the incircle radius or apothem, a, of a regular hexagon with area (A_{hex}) equal to the area of the leaf (A_l) divided by the number of stomata (n_{stomata}) on the leaf according to Eq. 4:

$$s = \frac{\sqrt{2}}{3^{1/4}\sqrt{n_{\text{stomata}}/A_l}} \tag{4}$$

As all sides of an equilateral triangle have the same length, the average nearest neighbor distance for a given D_S is maximized and each stomate occupies the same hexagonal area (A_{hex}). The closer to one DI is, the more uniform an area each of its stomata supply with CO_2 during photosynthesis. We tested whether light treatment affects DI and D_S using analysis of variance (ANOVA).

Finally, to test our hypothesis that stomatal length is modulated by the area of the leaf to which it supplies CO_2, we examined the relationship between stomatal zone area and stomatal length using a Bayesian generalized non-linear multilevel model with the R package **brms** version 2.20.1. Stomatal zone area was calculated using voronoi tessellation (e.g. Fig. 3). The stomatal zone area, S_{area}, is the region of the leaf surface whose distance to stomate, S, is less than the distance to any other stomate, S. Stomatal length was measured in `ImageJ` (Schneider, Rasband, and Eliceiri 2012).

2.3 Paired Abaxial and Adaxial Surface Analysis

To test whether the position of ab- and adaxial stomata are coordinated we compared the observed distribution to a null distribution where the positions on each surface are random. For each pair of surfaces (observed or synthetic) we calculated the distance squared between each to the nearest stomatal centroid with the R package **raster** version 3.6.23. Then we calculated the cell-wise Pearson correlation coefficient. If stomatal positions on each surface are coordinated to minimize the distance between mesophyll and the nearest stomate, then we expect a negative correlation. A cell that is far from a stomate on one surface should be near a stomate on the other surface (Fig. 5). We

generated a null distribution of the correlation coefficient by simulating 10^3 synthetic data sets for each observed pair. For each synthetic data set, we simulated stomatal position using a random uniform distribution, as described above, matching the number of stomata on abaxial and adaxial leaf surfaces. Stomatal positions on each surface are coordinated if the correlation coefficient is greater than 95% of the synthetic correlation values (one-tailed test).

2.4 Modeling Photosynthesis

We modeled photosynthesis CO_2 assimilation rate using a spatially-explicit two-dimensional reaction diffusion model using a porous medium approximation (Parkhurst 1994). Consider a two-dimensional leaf where stomata occur on each surface in a regular sequence with interstomatal distance U. The main outcome we assessed is the advantage of offsetting the position of stomata on each surface compared to have stomata on the same x position on each surface. With these assumptions, by symmetry, we only need to model two stomata, one abaxial and one adaxial, from $x = 0$ to $x = U/2$ and from the adaxial surface at $y = 0$ to the abaxial surface at $y = L$, the leaf thickness. We arbitrarily set the adaxial stomate at $x = 0$ and toggled the abaxial stomata position between $x = U/2$ (offset) or $x = 0$ (below adaxial stomate). The advantage of offsetting stomatal position on each surface is the photosynthetic rate of the leaf with offset stomata compared to that with stomata aligned in the same x position:

$$\text{coordination advantage} = \frac{A_{\text{offset}}}{A_{\text{aligned}}} \tag{5}$$

We modelled the coordination advantage over a range of leaf thicknesses, stomatal densities, photosynthetic capacities, and light environments to understand when offsetting stomatal position on each surface might deliver a significant photosynthetic advantage.

2.4.1 Light propogation model

[NOTE: we should probably adjust light attenuation to be proportional to the chlorophyll concentration which is one of the parameters in the biochemical models.]

Irradiance at depth y in a leaf with thickness L is modeled following Lloyd *et al.* (1992):

$$I(y) = 1.1 I_0 e^{-2.4y/L} \tag{6}$$

where I_0 is photosynthetically active irradiance incident on the adaxial leaf surface.

2.4.2 Biochemical model

All parameter symbols, units, descriptions, and values are described in Table X below. Following Gutschick (1984), we modeled photosynthetic rate per unit chlorophyll A_{chl} then calculated the volumetric photosynthetic rate A_{volume} by multiplying by the chlorophyll concentration Q_{chl}:

$$A_{\text{volume}} = A_{\text{chl}} Q_{\text{chl}}$$

A description of the model is given on page 553-556 of Gutschick (1984). The R code below is how we implemented the model.

- `C_m` is a vector CO_2 concentrations in mmol m^{-3} at different positions within the leaf
- `I_m` is a vector of irradiances in μmol m^{-2}s^{-1} at different positions within the leaf (same order as `C_m`).
- `pars` is a list of parameters

```r
pars = list(

  P = set_units(101.325, kPa), # air pressure at sea level
  temp = set_units(298.15, K), # assume constant temperature
  R_gas = set_units(8.314, J/K/mol), # ideal gas constant


  # Calculations for C_a and O ued below
  # 21% O2
  # set_units(0.21 * P / (R_gas * temp), mol/m^3)
  # 415 ppm
  # set_units((415/1e6) * P / (R_gas * temp), mmol/m^3)


  # Environmental
  C_a = set_units(16.96367, mmol/m^3),
  O = set_units(8.584027, mol/m^3),
  PAR = set_units(1000, umol/m^2/s),


  # Biochemical
  E_t = set_units(0.01, mol/mol),
  eta_t = set_units(0.59, 1),
  k_c = set_units(20, mol/mol/s),
  k_o = set_units(4.2, mol/mol/s),
```

```r
    K_c = set_units(0.0184, mol/m^3),
    K_o = set_units(13.2, mol/m^3),
    Q_chl = set_units(3.3, mol/m^3),
    R_p = set_units(0.273, mol/mol),


    # Diffusivity of CO2 in leaf airspace. From Gutschick 1984. Should be updated an
    D_mc = set_units(7e-7, m^2/s)


)


# strip units to speed up calculation
upars = purrr::map(pars, ~ {if(inherits(.x, "units")) {drop_units(.x)}})


# multiply/divide by 1e3 because C_m is mmol and parameters are in mol
k_vc = upars[["k_c"]] / (1 + (1e3 * upars[["K_c"]] / C_m) *
                           (1 + upars[["O"]] / upars[["K_o"]])) # [1/s]
# Given light_propagation assumptions, k = 2.4/L assuming no scattering
k_i = 2.4 / upars[["leaf_thickness"]] # [1/um] # I'm not sure sure this is right
b_x = k_i * I_m # [mol/m^3/s]
a_x = b_x / upars[["Q_chl"]] # [1/s]
j = 0.5 * a_x * upars[["eta_t"]] # [1/s] # eqn 9
phi = upars[["k_o"]] / upars[["k_c"]] * (upars[["O"]] / upars[["K_o"]]) /
  (1e-3 * C_m / upars[["K_c"]]) # [1]
v_cj = j / (4 + 4 * phi) # [1/s]
v_cp = k_vc * upars[["R_p"]] # [1/s]
v_cr = apply(cbind(v_cj, v_cp), 1, min) # [1/s]
v_c = apply(cbind(k_vc * upars[["E_t"]], v_cr), 1, min) # [1/s]
v_o = phi * v_c # [1/s]
A_chl = v_c - 0.5 * v_o # [1/s] # i.e mol CO2 / mol Chl / s
A_volume = A_chl * upars[["Q_chl"]] # [mol/m^3/s]
```

238   To model photosynthesis and CO_2 transport within a two-dimensional cross section
239 of the leaf, we built a grid of nodes of dimensions leaf thickness by half the interstomatal
240 distance. Nodes represent the leaf mesophyll where CO_2 diffusion and assimilation occur.
241   **Table X** Glossary of mathematical symbols. The columns indicate the mathematical
242 Symbol used in the paper, the associated symbol used in R scripts, scientific Units, and
243 a verbal Description.

Symbol	Value(s)	Units	Description
Biochemical Parameters			
A_{volume}	NA	$molCO_2/m^3/s$	volumetric assimilation rate
A_{chl}	NA	$molCO2/molChl/s$	assimilation rate per mol chlorophyll
E_t	0.01	$mol/molChl$	rubisco octamer concentration per chlorophyll
eta_t	0.59	unitless	quantum efficiency of photoexcitation transfer to reaction centers
k_c	20	$molCO2/molRubisco/s$ at 25 C	maximal carboxylation velocity of Rubisco
k_o	4.2	$molO2/molRubisco/s$ at 25 C	maximal oxygenation velocity of Rubisco
K_c	0.0184	mol/m^3 at 25 C	Michaelis constant for CO2
K_o	13.2	mol/m^3 at 25 C	Michaelis constant for O2
J_{max}	0.253	$mole\text{-}/molChl/s$	maximal electron transport rate per mol Chl
Q_{chl}	3.3	mol/m^3	Chl volume concentration
v_c	NA	$molCO2/molChl/s$	carboxylation rate
v_o	NA	$molO2/molChl/s$	oxygenation rate
k_{vc}	NA	$molCO2/molRubisco/molChl$	carboxylation velocity per Rubisco octamer at ambient CO2
R_p	0.273	$molRuBP/molChl$	RuBP pool size
k_i	2.4	$1/m^2$ or $1/L$	light attenuation coefficient
D_{mc}	7e-7	m^2/s	diffusivity of CO_2 in mesophyll airspace
Environmental Parameters			
P	101.325	kPa	air pressure at sea level
$temp$	298.15	K	temperature
R_{gas}	8.314	$J/K/mol$	ideal gas constant
C_a	16.96367	$mmolCO_2/m^3$	atmospheric CO_2 concentration
O	8.584027	$molO_2/m^3$	atmospheric O_2 concentration
PAR	1000	$umolphotons/m^2/s$	photosynthetically active radiation

Symbol	Value(s)	Units	Description
Variables			
U_s	.05, .10, .15…	mm	interstomatal distance
T_l	.1, .2, .3…	mm	leaf thickness
g_{sc}	0.2, 0.3, 0.4…	$mol/m^2/s$	stomatal conductance

2.5   Two-dimensional model

FYI - something is wrong with the model. I think the units are off somewhere because the result is very sensitive to grid size and the values often aren't reasonable. I'll need to troubleshoot more, but maybe something will be obvious to you.

We used the `steady.2D()` function in the R package **rootSolve**. The function needs a function to calculate the time differential for node ij, $\frac{dC_{m,ij}}{dt}$. The R function below uses the light propagation, biochemical, and diffusional model to calculate a matrix of $\frac{dC_{m,ij}}{dt}$ values:

```r
diffusion2D <- function (time, state, pars, stomata_offset) {

  n_row = pars[["n_row"]]
  n_col = pars[["n_col"]]


  n_node = n_row * n_col


  node_length_m = node_length * 1e-6 # node_length in [m]


  # matrix of C_m values
  C_m_mat = matrix(nrow = n_row, ncol = n_col, state)


  # Photosynthetic demand
  ## Light matrix
  I_mat = seq(0, by = pars[["node_length"]], length.out = n_row) |>
    light_propogation(pars[["leaf_thickness"]], pars[["PAR"]]) |>
    matrix(n_row, ncol = n_col)


  ## Biochemical model
```

```r
  # Units have to be correct for this to work, but unitless = TRUE should be faster
  A = biochemical_model(C_m_mat, I_mat, pars = pars, unitless = TRUE)


  ## Photosynthesis matrix
  ## multiply by 1000 to convert from mol / m^3 / s to mmol / m^3 / s
  A_mat = matrix(nrow = n_row, ncol = n_col, 1e3 * A)


  # CO2 diffusion
  C_a = drop_units(pars[["C_a"]])
  flux_mat = matrix(nrow = n_row, ncol = n_col, 0)
  flux_mat[1, 1] = pars[["g_sc"]] * (C_a - C_m_mat[1, 1])


  ## 1. Flux through stomata
  if (stomata_offset) {
    flux_mat[n_row, n_col] = pars[["g_sc"]] * (C_a - C_m_mat[n_row, n_col])
  } else {
    flux_mat[n_row, 1] = pars[["g_sc"]] * (C_a - C_m_mat[n_row, 1])
  }


  zero_x <- rep(0, n_row)
  zero_y <- rep(0, n_col)


  ## 2. Mesophyll flux; zero fluxes near boundaries
  flux_above = rbind(rep(0, n_col), C_m_mat[1:(n_row - 1), ] - C_m_mat[2:n_row, ])
  flux_below = rbind(C_m_mat[2:n_row, ] - C_m_mat[1:(n_row - 1), ], rep(0, n_col))
  flux_left  = cbind(rep(0, n_col), C_m_mat[, 1:(n_col - 1)] - C_m_mat[, 2:n_col])
  flux_right = cbind(C_m_mat[, 2:n_col] - C_m_mat[, 1:(n_col - 1)], rep(0, n_col))


  # g_mc [m/s] = D_mc [m^2/s] / node_length [m]
  flux_mat = flux_mat + pars[["g_mc"]] * (flux_above + flux_below + flux_left + flux_

    return(list(c(as.vector(flux_mat / node_length_m - A_mat))))


}
```

2.6   Global Results

Stomatal density of *Arabidopsis thaliana* the 132 leaves measured ranged from 12 to 93
(units) with high light leaves ranging from 93 to 55 (units), medium light from 15 to 35

(units), and low light from 12 to 42 (units). Leaves were amphistomatous with a mean stomatal ratio of 0.45.

2.7 Single Surface Results

If our hypotheses that natural selection will act to reduce the diffusion path length of CO_2 while minimizing stomatal number are correct, then we would expect to find leaf surfaces with uniformly distributed stomata. However, to the contrary, we find that though 57 of the 132 (43.1%) leaf surfaces were significantly more uniformly dispersed than uniform random synthetic stomatal grids ($\alpha = 0.05$), none of the leaf surfaces exhibited perfectly uniform stomatal patterning (dispersion index = 1) (Fig. 1). Additionally, we hypothesized that as CO_2 is more limiting to photosynthesis under high light, stomata would be more uniformly dispersed in plants grown in high light than plants grown in low and medium light. The data also fail to support this hypothesis as there is no strong, discernible trend between light and stomatal patterning. Interestingly, adaxial leaf surfaces were more uniformly dispersed than associated abaxial leaf surfaces across all light treatments ($F_{1,126} = 28.8$; p-value < 0.001). Rather than regulate stomatal patterning in response to light regimes, plants respond by increasing stomatal density (Fig. 2). Stomatal density drastically increased in plants grown under high light, validating the long held hypothesis that light strongly influences stomatal density ($F_{2,126} = 680.7$; p-value < 0.001).

Across all light treatments and leaf surfaces, stomatal length and stomatal area were weakly positively correlated, indicating some support for our hypothesis that stomata are selected for an optimal operational aperture (Fig. 4).

2.8 Dual Surface Analysis

As evidence against our hypothesis that natural selection should favor spatial coordination in the placement of stomata between abaxial and adaxial leaf surfaces, we found no correlation between paired abaxial and adaxial leaf surfaces (Fig. 6). Light treatment had no effect on correlation between surfaces ($F_{2,63} = 2.28$; p-value = 0.11). All but one abaxial, adaxial surface pairs were independent ($\alpha = 0.05$).

2.8.1 Example output

We wrapped the above functions to adjust environmental and anatomical variables. We're going to simulate over a grid of parameters, but here is what the output looks like plotted:

13

2.8.2 DRAFT TEXT

During a model run, CO_2 flux between neighboring nodes was determined according to the mesophyll CO_2 concentration (C_m) in each node, distance between cells, temperature, pressure, and leaf porosity. Assimilation rate (A) in each node was determined by A_{max}, c_i, irradiance, temperature, chlorophyll volume concentration, Rubisco octamer concentration per mol chlorophyll, and maximal oxygenation and carboxylation rates of Rubisco. Stomata were placed either 1) directly on top of one another to represent anticoordination or 2) offset from one another to represent coordination between leaf surfaces. c_i and CO_2 assimilation rate (A) were set to 415ppm and 0 respectively and the model ran until c_i and A reached equilibrium in each cell. Total A and average c_i were then calculated for each parameter combination.

A was calculated in terms of A_{max} and c_i following Eq. 7

$$A = A_{max} * c_i / (c_i + K_c) \tag{7}$$

where K_c is the Michaelis constant for CO_2: 0.0184 mol m^{-3}.

A_{max} was calculated in terms of irradiance (i), light saturated maximum A (A_{mm}), and quantum yield (φ) following Eq. 8

$$A_{max} = A_{mm} * \varphi * i / (A_{mm} + \varphi * i) \tag{8}$$

3 Results

3.1 Single surface analysis

3.2 Dual surface analysis

4 Discussion

Stomata are expensive. A theoretical, optimized plant would minimize stomatal density while also allowing competitive gas exchange rates for its environment so as to maximize C assimilation per unit investment in stomata. Natural selection operates within developmental and physical constraints to drive each plant species toward its theoretical optimum. This study provides evidence that stomata in *Arbidopsis thaliana*, the model angiosperm, are non-randomly distributed, favoring dispersion over clustering (Fig. 1). However, stomata are not ideally dispersed in an equilateral triangular grid as would be optimal to minimize CO_2 diffusion path length and standardize the area supplied by each stomate (Fig. 3). Additionally, when grown in high light environments, *A. thaliana* exhibited increased stomatal density rather than increased stomatal dispersion (Fig. 2),

which suggests that natural selection has acted more strongly on developmental pathways that modulate stomatal density than those that control stomatal dispersion. In other words, plants optimize gas exchange by adding more stomata rather than dispersing them more evenly across the leaf surface. This study also demonstrates that stomata that supply larger leaf areas with CO_2 tend to be larger (Fig. 4). These results could suggest that 1) the added energetic and hydraulic cost of non-ideally dispersed stomata is negligible and therefore not acted on by natural selection; 2) no developmental pathway exists to ensure the ideal placement of stomata on the leaf; or 3) the regulation of stomatal size limits the cost incurred by non-ideal stomatal dispersion.

In high light environments, amphistomy is favorable as high light photosynthesis is limited by CO_2 and amphistomy halves diffusion path length and boundary layer resistance, thereby reducing CO_2 limitation - increasing theoretical A_{max}. An optimal amphistomatous leaf has offset stomata such that stomata are more likely to appear on one leaf surface if there is not a stomata directly opposite it on the other surface as shown in figure 5. However, our results show that leaf surfaces are not coordinated but are independent, regardless of light (Fig. 6). Additionally, gas exchange models show little photosynthetic efficiency gain from abaxial-adaxial stomatal coordination compared to anticoordination (INSERT FIG FROM MODELING). We posit that this marginal gain is not sufficient to be acted upon strongly by natural selection. Thus, amphistomatous plants do not exhibit abaxial-adaxial stomatal coordination for there is little selective advantage of it.

Our study corroborates previous studies which demonstrate that stomata are non-randomly distributed along the leaf surface as a result of developmental mechanisms such as spatially biased arrest of stomatal initials (Boetsch, Chin, and Croxdale 1995), oriented asymmetric cell division (Geisler, Nadeau, and Sack 2000), and cell cycle controls (Croxdale 2000). We do not investigate the potential developmental pathways that influence stomatal dispersion in this study; however, they are important to consider as these pathways could limit plants from reaching the theoretical peak in the adaptive landscape: uniform stomatal dispersion. Instead, as this study suggests, plants may simply compensate with higher stomatal density and by fitting stomatal size to the area that they supply with CO_2. To understand why stomata are not ideally dispersed, more modelling should be done to estimate the fitness gain of stomatal dispersion. Additionally, genetic manipulation studies should attempt to create mutants with clustered and ideally dispersed stomata for a comparison of their photosynthetic traits. This could have extremely important implications for maximum assimilation rates in crops as most crop species are grown in high light where CO_2 is often limiting. In drought-prone environments, increased stomatal dispersion may increase water use efficiency by reducing the number of stomata needed to achieve the same internal CO_2 concentration, C_i.

Beyond disperson on a single surface, gas exchange can be optimized via stomatal

15

coordination of abaxial and adaxial surfaces in amphistomatous leaves. Given that leaf thicknesses are generally multiple times greater than interstomatal distance (GIVE DISTANCES HERE). As a result, abaxial-adaxial stomatal coordination reduces CO_2 diffusion path length far less than single surface dispersion, so we hypothesize this strategy to afford less photosynthetic advantage to the leaf. Our modelling results demonstrate that, even in ideal conditions, i.e. thick leaf, low stomatal densities, high light, low leaf porosity, high rubisco concentration, etc., the photosynthetic advantage of coordination is minimal. We are not surprised by these results, but still highlight them here as we are the first to report this finding.

Amphistomy is a unique and important adaptation found around the world across many plant lineages (Christopher D. Muir 2018), yet much of the dynamics of amphistomy remain poorly understood. Here, we show that in *Arabidopsis thaliana* 1) stomata in are non-randomly dispersed, but not ideally dispersed; 2) stomatal size and density are modulated by light; 3) stomatal size is positively correlated with the area to which it supplies CO_2; and 4) abaxial-adaxial stomatal coordination is not exhibited and is not shown to provide a strong photosynthetic advantage using CO_2 diffusion models. Interestingly, these findings did not validate many of our hypotheses which were based on first principles, suggesting that there may be limits on plants' ability to control stomatal placement. Future studies which elucidate these limitations may have important implications for agriculturaly productivity in a rapidly changing world.

References

Aalto, T., and E. Juurola. 2002. "A Three-Dimensional Model of CO $_2$ Transport in Airspaces and Mesophyll Cells of a Silver Birch Leaf: CO $_2$ Transport Inside a Birch Leaf." *Plant, Cell & Environment* 25 (11): 1399–409. `https://doi.org/10.1046/j.0016-8025.2002.00906.x`.

Boetsch, John, Jonathan Chin, and Judith Croxdale. 1995. "Arrest of Stomatal Initials in Tradescantia Is Linked to the Proximity of Neighboring Stomata and Results in the Arrested Initials Acquiring Properties of Epidermal Cells." *Developmental Biology* 168 (1): 28–38. `https://doi.org/10.1006/dbio.1995.1058`.

Buckley, Thomas N, Lawren Sack, and Graham D Farquhar. 2017. "Optimal Plant Water Economy." *Plant, Cell & Environment* 40 (6): 881–96. `https://doi.org/10.1111/pce.12823`.

Büssis, Dirk, Uritza von Groll, Joachim Fisahn, and Thomas Altmann. 2006. "Stomatal Aperture Can Compensate Altered Stomatal Density in Arabidopsis Thaliana at Growth Light Conditions." *Functional Plant Biology* 33 (11): 1037. `https://doi.org/10.1071/FP06078`.

Camargo, Miguel Angelo Branco, and Ricardo Antonio Marenco. 2011. "Density, Size

and Distribution of Stomata in 35 Rainforest Tree Species in Central Amazonia." *Acta Amazonica* 41 (2): 205–12. `https://doi.org/10.1590/S0044-59672011000200004`.

Carriquí, M., H. M. Cabrera, M. À. Conesa, R. E. Coopman, C. Douthe, J. Gago, A. Gallé, et al. 2015. "Diffusional Limitations Explain the Lower Photosynthetic Capacity of Ferns as Compared with Angiosperms in a Common Garden Study: Photosynthetic Comparison in Ferns and Angiosperms." *Plant, Cell & Environment* 38 (3): 448–60. `https://doi.org/10.1111/pce.12402`.

Cowan, IR, and GD Farquhar. 1977. "Stomatal Function in Relation to Leaf Metabolism and Environment." *STOMATAL FUNCTION IN RELATION TO LEAF METABOLISM AND ENVIRONMENT.*

Croxdale, Judith L. 2000. "Stomatal Patterning in Angiosperms." *American Journal of Botany* 87 (8): 1069–80. `https://doi.org/10.2307/2656643`.

Deans, Ross M., Timothy J. Brodribb, Florian A. Busch, and Graham D. Farquhar. 2020. "Optimization Can Provide the Fundamental Link Between Leaf Photosynthesis, Gas Exchange and Water Relations." *Nature Plants* 6 (9): 1116–25. `https://doi.org/10.1038/s41477-020-00760-6`.

Dow, Graham J., Joseph A. Berry, and Dominique C. Bergmann. 2014. "The Physiological Importance of Developmental Mechanisms That Enforce Proper Stomatal Spacing in *<Span Style="font-Variant:small-Caps;">A</Span> Rabidopsis Thaliana*." *New Phytologist* 201 (4): 1205–17. `https://doi.org/10.1111/nph.12586`.

Drake, Paul L., Hugo J. Boer, Stanislaus J. Schymanski, and Erik J. Veneklaas. 2019. "Two Sides to Every Leaf: Water and <Span Style="font-Variant:small-Caps;">CO</Span>$_2$ Transport in Hypostomatous and Amphistomatous Leaves." *New Phytologist* 222 (3): 1179–87. `https://doi.org/10.1111/nph.15652`.

Earles, J. Mason, Guillaume Theroux-Rancourt, Adam B. Roddy, Matthew E. Gilbert, Andrew J. McElrone, and Craig R. Brodersen. 2018. "Beyond Porosity: 3D Leaf Intercellular Airspace Traits That Impact Mesophyll Conductance." *Plant Physiology* 178 (1): 148–62. `https://doi.org/10.1104/pp.18.00550`.

Evans, J. R., R. Kaldenhoff, B. Genty, and I. Terashima. 2009. "Resistances Along the CO_2 Diffusion Pathway Inside Leaves." *Journal of Experimental Botany* 60 (8): 2235–48. `https://doi.org/10.1093/jxb/erp117`.

Farquhar, G. D., S. von Caemmerer, and J. A. Berry. 1980. "A Biochemical Model of Photosynthetic CO2 Assimilation in Leaves of C3 Species." *Planta* 149 (1): 78–90. `https://doi.org/10.1007/BF00386231`.

Franks, Peter J., Ilia J. Leitch, Elizabeth M. Ruszala, Alistair M. Hetherington, and David J. Beerling. 2012. "Physiological Framework for Adaptation of Stomata to CO$_2$ from Glacial to Future Concentrations." *Philosophical Transactions of the Royal Society B: Biological Sciences* 367 (1588): 537–46. `https://doi.org/10.1098/rstb.2011.0270`.

Gay, A. P., and R. G. Hurd. 1975. "THE INFLUENCE OF LIGHT ON STOMATAL DENSITY IN THE TOMATO." *New Phytologist* 75 (1): 37–46. `https://doi.org/10.1111/j.1469-8137.1975.tb01368.x`.

Geisler, Matt, Jeanette Nadeau, and Fred D. Sack. 2000. "Oriented Asymmetric Divisions That Generate the Stomatal Spacing Pattern in Arabidopsis Are Disrupted by the *Too Many Mouths* Mutation." *The Plant Cell* 12 (11): 2075–86. `https://doi.org/10.1105/tpc.12.11.2075`.

Harrison, Emily L., Lucia Arce Cubas, Julie E. Gray, and Christopher Hepworth. 2020. "The Influence of Stomatal Morphology and Distribution on Photosynthetic Gas Exchange." *The Plant Journal* 101 (4): 768–79. `https://doi.org/10.1111/tpj.14560`.

Harwood, Richard, Guillaume Théroux-Rancourt, and Margaret M Barbour. 2021. "Understanding Airspace in Leaves: <Span Style="font-Variant:small-Caps;">3D</Span> Anatomy and Directional Tortuosity." *Plant, Cell & Environment*, May, pce.14079. `https://doi.org/10.1111/pce.14079`.

Jordan, Gregory J., Raymond J. Carpenter, and Timothy J. Brodribb. 2014. "Using Fossil Leaves as Evidence for Open Vegetation." *Palaeogeography, Palaeoclimatology, Palaeoecology* 395 (February): 168–75. `https://doi.org/10.1016/j.palaeo.2013.12.035`.

Jordan, Gregory J., Raymond J. Carpenter, Anthony Koutoulis, Aina Price, and Timothy J. Brodribb. 2015. "Environmental Adaptation in Stomatal Size Independent of the Effects of Genome Size." *New Phytologist* 205 (2): 608–17. `https://doi.org/10.1111/nph.13076`.

Kaiser, Elias, Alejandro Morales, Jeremy Harbinson, Ep Heuvelink, Aina E. Prinzenberg, and Leo F. M. Marcelis. 2016. "Metabolic and Diffusional Limitations of Photosynthesis in Fluctuating Irradiance in Arabidopsis Thaliana." *Scientific Reports* 6 (1): 31252. `https://doi.org/10.1038/srep31252`.

Lange, O. L., R. L sch, E. -D. Schulze, and L. Kappen. 1971. "Responses of Stomata to Changes in Humidity." *Planta* 100 (1): 76–86. `https://doi.org/10.1007/BF00386887`.

Lee, Richard, and David M. Gates. 1964. "Diffusion Resistance in Leaves as Related to Their Stomatal Anatomy and Micro-Structure." *American Journal of Botany* 51 (9): 963–75. `https://doi.org/10.1002/j.1537-2197.1964.tb06725.x`.

Lehmann, Peter, and Dani Or. 2015. "Effects of Stomata Clustering on Leaf Gas Exchange." *New Phytologist* 207 (4): 1015–25. `https://doi.org/10.1111/nph.13442`.

Lehmeier, Christoph, Radoslaw Pajor, Marjorie R. Lundgren, Andrew Mathers, Jen Sloan, Marion Bauch, Alice Mitchell, et al. 2017. "Cell Density and Airspace Patterning in the Leaf Can Be Manipulated to Increase Leaf Photosynthetic Capacity." *The Plant Journal* 92 (6): 981–94. `https://doi.org/10.1111/tpj.13727`.

Liu, Congcong, Christopher D. Muir, Ying Li, Li Xu, Mingxu Li, Jiahui Zhang, Hugo Jan de Boer, et al. 2021. "Scaling Between Stomatal Size and Density in Forest Plants." Preprint. Plant Biology. `https://doi.org/10.1101/2021.04.25.441252`.

Manter, D. K. 2004. "A/Ci Curve Analysis Across a Range of Woody Plant Species: Influence of Regression Analysis Parameters and Mesophyll Conductance." *Journal of Experimental Botany* 55 (408): 2581–88. `https://doi.org/10.1093/jxb/erh260`.

McAdam, Scott A. M., and Timothy J. Brodribb. 2016. "Linking Turgor with ABA Biosynthesis: Implications for Stomatal Responses to Vapor Pressure Deficit Across Land Plants." *Plant Physiology* 171 (3): 2008–16. `https://doi.org/10.1104/pp.16.00380`.

Morison, James I. L., Emily Gallouët, Tracy Lawson, Gabriel Cornic, Raphaèle Herbin, and Neil R. Baker. 2005. "Lateral Diffusion of CO <Sub>2<sub> in Leaves Is Not Sufficient to Support Photosynthesis." *Plant Physiology* 139 (1): 254–66. `https://doi.org/10.1104/pp.105.062950`.

Mott, Keith A., Arthur C. Gibson, and James W. O'Leary. 1982. "The Adaptive Significance of Amphistomatic Leaves." *Plant, Cell & Environment* 5 (6): 455–60. `https://doi.org/10.1111/1365-3040.ep11611750`.

Mott, Keith A., and Odette Michaelson. 1991. "AMPHISTOMY AS AN ADAPTATION TO HIGH LIGHT INTENSITY IN AMBROSIA CORDIFOLIA (COMPOSITAE)." *American Journal of Botany* 78 (1): 76–79. `https://doi.org/10.1002/j.1537-2197.1991.tb12573.x`.

Muir, Christopher D. 2019. "Is Amphistomy an Adaptation to High Light? Optimality Models of Stomatal Traits Along Light Gradients." *Integrative and Comparative Biology* 59 (3): 571–84. `https://doi.org/10.1093/icb/icz085`.

Muir, Christopher D. 2018. "Light and Growth Form Interact to Shape Stomatal Ratio Among British Angiosperms." *New Phytologist* 218 (1): 242–52. `https://doi.org/10.1111/nph.14956`.

Muir, Christopher D., Miquel Àngel Conesa, Jeroni Galmés, Varsha S. Pathare, Patricia Rivera, Rosana López Rodríguez, Teresa Terrazas, and Dongliang Xiong. 2023. "How Important Are Functional and Developmental Constraints on Phenotypic Evolution? An Empirical Test with the Stomatal Anatomy of Flowering Plants." *The American Naturalist* 201 (6): 794–812. `https://doi.org/10.1086/723780`.

Murray, Michelle, Wuu Kuang Soh, Charilaos Yiotis, Robert A. Spicer, Tracy Lawson, and Jennifer C. McElwain. 2020. "Consistent Relationship Between Field-Measured Stomatal Conductance and Theoretical Maximum Stomatal Conductance in C_3 Woody Angiosperms in Four Major Biomes." *International Journal of Plant Sciences* 181 (1): 142–54. `https://doi.org/10.1086/706260`.

Papanatsiou, Maria, Anna Amtmann, and Michael R. Blatt. 2017. "Stomatal Clustering in Begonia Associates with the Kinetics of Leaf Gaseous Exchange and Influences

Water Use Efficiency." *Journal of Experimental Botany* 68 (9): 2309–15. `https://doi.org/10.1093/jxb/erx072`.

Parkhurst, David F. 1978. "The Adaptive Significance of Stomatal Occurrence on One or Both Surfaces of Leaves." *Journal of Ecology* 66 (2): 367–83. `https://doi.org/10.2307/2259142`.

———. 1994. "Diffusion of CO_2 and Other Gases Inside Leaves." *New Phytologist* 126 (3): 449–79. `http://www.jstor.org/stable/2557929`.

Parkhurst, David F., and Keith A. Mott. 1990. "Intercellular Diffusion Limits to CO_2 Uptake in Leaves: Studies in Air and Helox." *Plant Physiology* 94 (3): 1024–32. `https://doi.org/10.1104/pp.94.3.1024`.

Pieruschka, R. 2005. "Lateral Gas Diffusion Inside Leaves." *Journal of Experimental Botany* 56 (413): 857–64. `https://doi.org/10.1093/jxb/eri072`.

Pieruschka, Roland, Ulrich Schurr, Manfred Jensen, Wilfried F. Wolff, and Siegfried Jahnke. 2006. "Lateral Diffusion of CO_2 from Shaded to Illuminated Leaf Parts Affects Photosynthesis Inside Homobaric Leaves." *New Phytologist* 169 (4): 779–88. `https://doi.org/10.1111/j.1469-8137.2005.01605.x`.

Roddy, Adam B., Guillaume Théroux-Rancourt, Tito Abbo, Joseph W. Benedetti, Craig R. Brodersen, Mariana Castro, Silvia Castro, et al. 2020. "The Scaling of Genome Size and Cell Size Limits Maximum Rates of Photosynthesis with Implications for Ecological Strategies." *International Journal of Plant Sciences* 181 (1): 75–87. `https://doi.org/10.1086/706186`.

Royer, D. L. 2001. "Stomatal Density and Stomatal Index as Indicators of Paleoatmospheric CO2 Concentration." *Review of Palaeobotany and Palynology* 114 (1-2): 1–28. `https://doi.org/10.1016/S0034-6667(00)00074-9`.

Sachs, T. 1974. "The Developmental Origin of Stomata Pattern in Crinum." *Botanical Gazette* 135 (4): 314–18. `https://doi.org/10.1086/336767`.

Sack, Lawren, and Thomas N. Buckley. 2016. "The Developmental Basis of Stomatal Density and Flux." *Plant Physiology* 171 (4): 2358–63. `https://doi.org/10.1104/pp.16.00476`.

Schneider, Caroline A, Wayne S Rasband, and Kevin W Eliceiri. 2012. "NIH Image to ImageJ: 25 Years of Image Analysis." *Nature Methods* 9 (7): 671–75. `https://doi.org/10.1038/nmeth.2089`.

Schoch, Paul-G., Claude Zinsou, and Monique Sibi. 1980. "Dependence of the Stomatal Index on Environmental Factors During Stomatal Differentiation in Leaves of *Vigna Sinensis* L.: 1. EFFECT OF LIGHT INTENSITY." *Journal of Experimental Botany* 31 (5): 1211–16. `https://doi.org/10.1093/jxb/31.5.1211`.

Sperry, John S., Martin D. Venturas, William R. L. Anderegg, Maurizio Mencuccini, D. Scott Mackay, Yujie Wang, and David M. Love. 2017. "Predicting Stomatal Responses to the Environment from the Optimization of Photosynthetic Gain and

Hydraulic Cost: A Stomatal Optimization Model." *Plant, Cell & Environment* 40 (6): 816–30. `https://doi.org/10.1111/pce.12852`.

Woodward, F. I. 1987. "Stomatal Numbers Are Sensitive to Increases in CO2 from Pre-Industrial Levels." *Nature* 327 (6123): 617–18. `https://doi.org/10.1038/327617a0`.

Yi Gan, Lei Zhou, Zhong-Ji Shen, Zhu-Xia Shen, Yi-Qiong Zhang, and Gen-Xuan Wang. 2010. "Stomatal Clustering, a New Marker for Environmental Perception and Adaptation in Terrestrial Plants." *Botanical Studies* 51 (3): 325–36. `https://search.ebscohost.com/login.aspx?direct=true&db=a9h&AN=60102322&site=ehost-live`.

Acknowledgements

List of Tables

	trait	relationship
1	leaf thickness	+
2	stomatal density	-
3	leaf porosity	-
4	lat.-vert. diffusion ratio	-
5	temperature	-
6	pressure	-
7	Rubisco concentration	+
8	light	+

Table 2: A summary of the hypothesized relationships between leaf traits and environmental conditions and photosynthetic advantage of stomatal spatial coordination in amphistomatous leaves.

List of Figures

Figure 1: Stomata are more dispersed than expected under the null model of uniform random position (dispersion index = 0) but far from a distribution that maximizes distance between stomata (dispersion index = 1). Significant differences between light treatments are indicated by asterisks according to analysis of variance followed by a post-hoc tukey honest significant difference test ($\alpha = 0.05$).
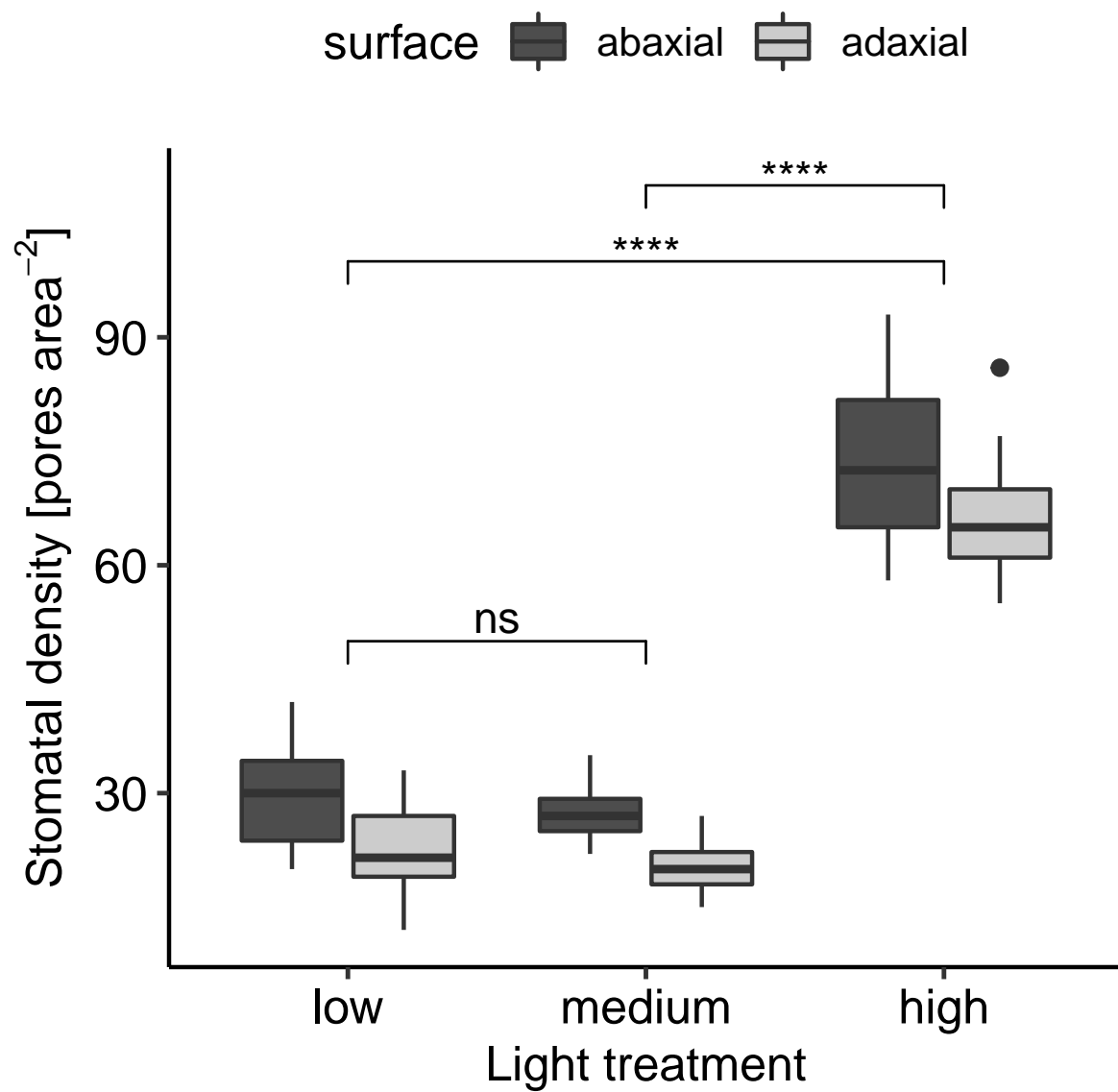
Figure 2: Stomatal density is higher in plants grown under high light conditions. Significant differences between light treatments are indicated by asterisks according to analysis of variance followed by a post-hoc tukey honest significant difference test ($\alpha = 0.05$).
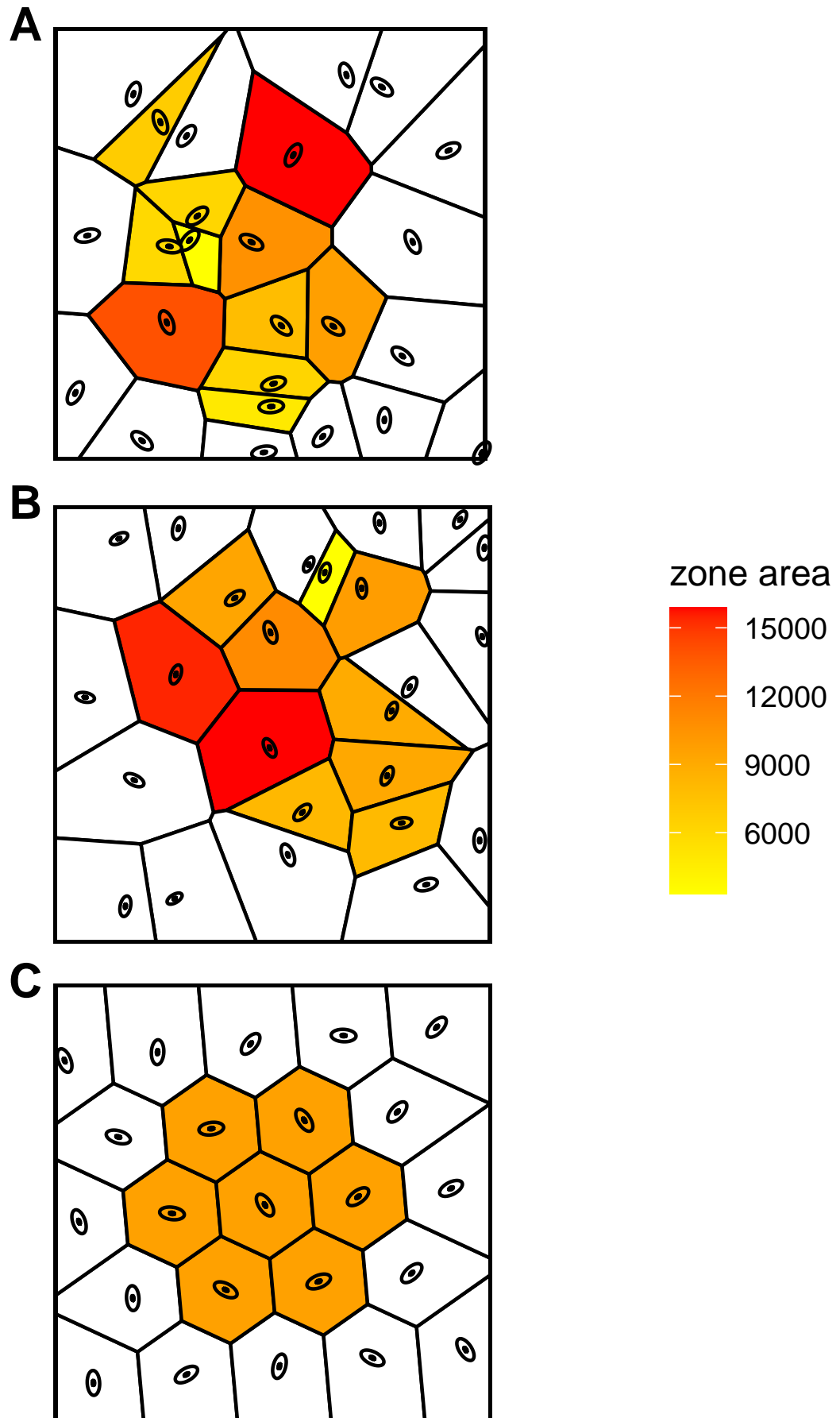
Figure 3: Examples of synthetic and real leaf surfaces. A) Uniform random synthetic leaf surface; B) Example of real leaf surface; C) Regularly distributed synthetic leaf surface. The zone defined by each stomate was calculated with voronoi tessellation and correlated with stomatal length in real leaves.
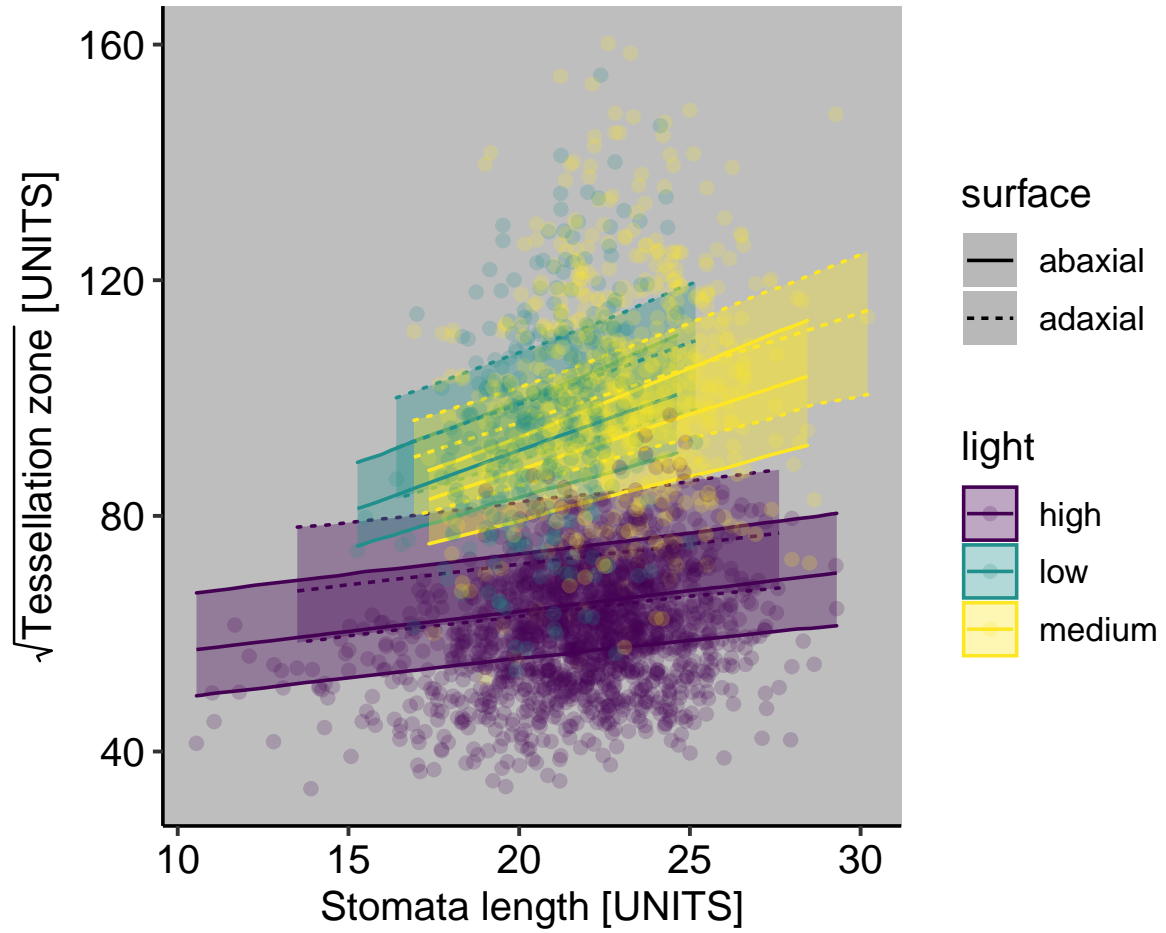
Figure 4: Stomatal length and stomatal zone area. Lines of best fit computed using a bayesian generalized non-linear multilevel model. Each light level and leaf surface exhibits a unique, weakly positive relationship between stomatal zone area and length.
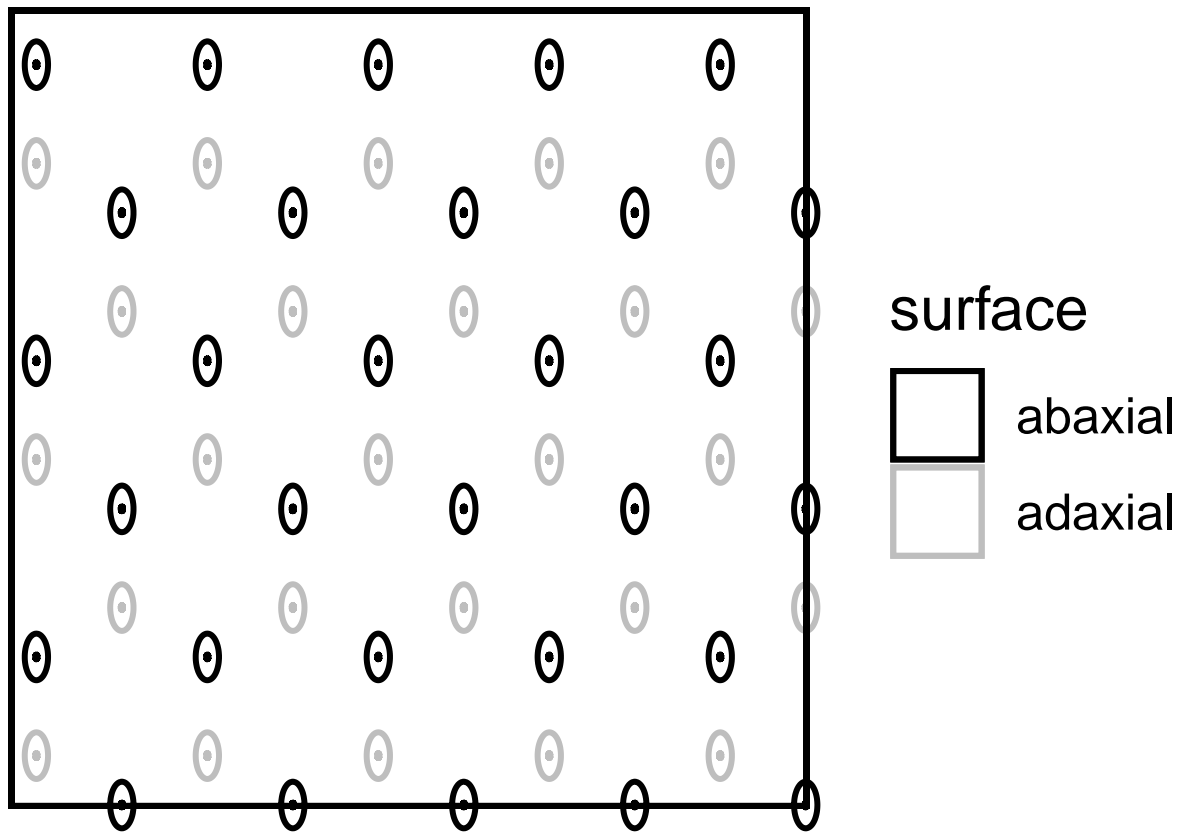
Ideal Stomatal Patterning

Figure 5: Idealized amphistomatous stomatal grid with uniform stomatal patterning and perfect abaxial-adaxial coordination.
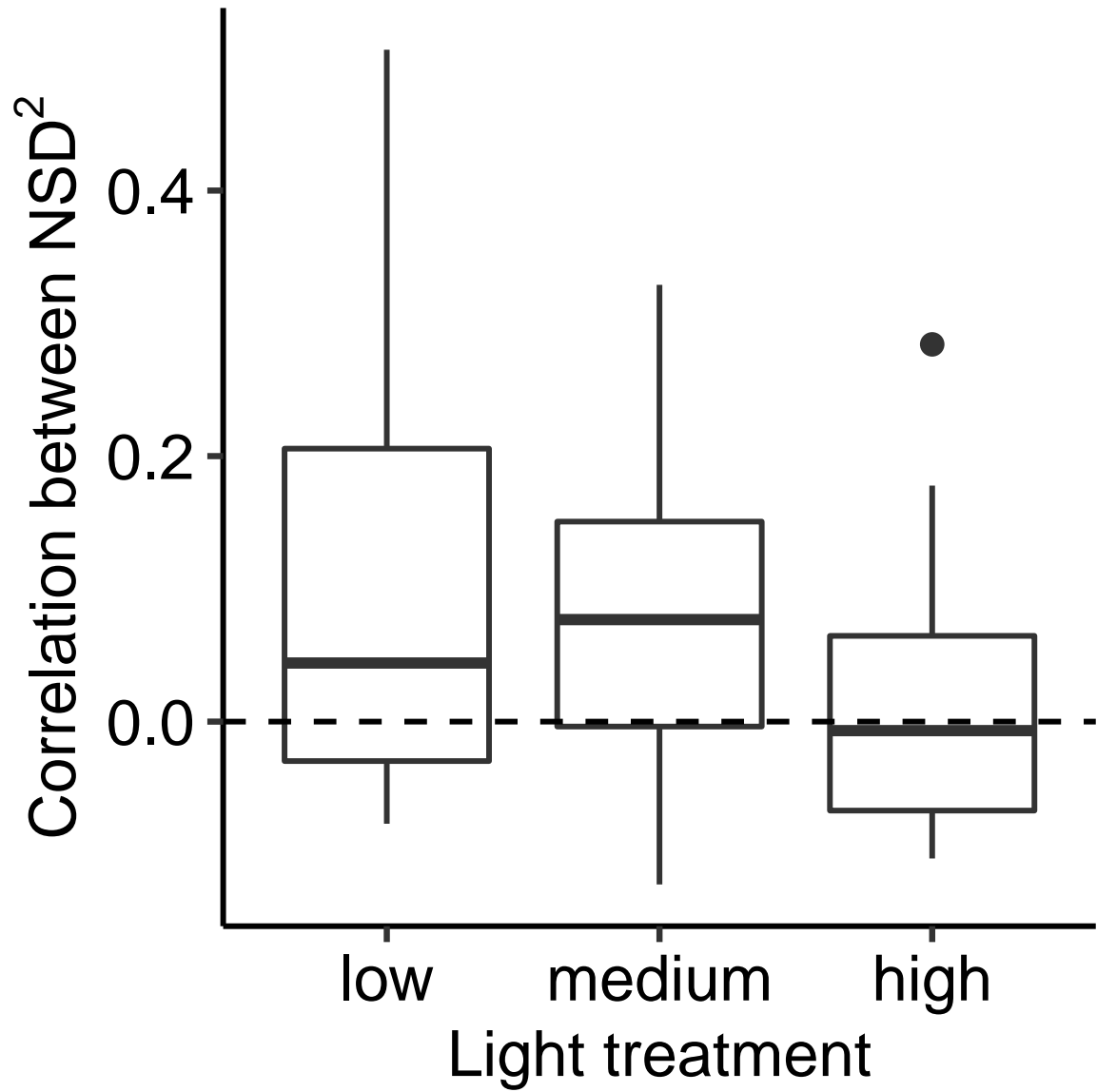
Figure 6: Correlation between paired abaxial and adaxial leaf surfaces. Dashed line indicates no correlation. Weak positive correlations are not significantly different from null simulations. No differences in abaxial-adaxial correlation were observed between light levels according to an analysis of variance ($\alpha = 0.05$).